Electrical Engineering (2025) 107:205–222
https://doi.org/10.1007/s00202-024-02513-6

ORIGINAL PAPER

An optimization based resilient control strategy for voltage unbalance compensation in grid connected microgrid system

Yadala Pavankumar[1] · Sudipta Debnath[1] · Subrata Paul[1]

Received: 16 July 2023 / Accepted: 29 May 2024 / Published online: 12 June 2024

Abstract

A novel two stage multi-objective control strategy for optimal voltage unbalance compensation in low voltage microgrid systems consisting of inverter interfaced distributed generators (IIDGs) has been presented in this research. To ensure continuous and safe operation of the IIDGs during unbalanced voltage sags, the proposed control strategy supplies the optimal positive sequence voltage support and performs voltage unbalance compensation considering the current limitation of the inverters. The control strategy also ensures that the DGs deliver maximum allowable active power during voltage sag. The positive and negative sequence quantities of the IIDGs are controlled in such a way so that these objectives can be achieved simultaneously. The DGs are operated in coordination with each other to maintain the voltage profile as desired by the grid operator. Prioritisation of active power and unbalance compensation can be set depending upon the requirement of the customer. Under severe grid imbalance condition, the proposed technique can raise the positive sequence voltage to near nominal value from below 0.9 per unit maintaining all phase currents of DGs within safety limit.To solve the optimization problem and to generate the optimal references for the DG control unit, artificial cooperative search algorithm has been utilised. The two stage control strategy includes a local control for each DG, which coordinates with the central control to provide the optimal references for all the DGs. The multi-objective control strategy has been tested under different operating conditions and implemented in real time digital simulator to ensure the robustness and effectiveness of the proposed approach.

Keywords Microgrid · Voltage unbalance compensation · Multi-objective control strategy · Artificial cooperative search algorithm

Abbrevations

PCC	Point of common coupling
VUF	Voltage unbalance factor
DG	Distributed generator
ACS	Artificial cooperative search algorithm
RES	Renewable energy sources
LVRT	Low voltage ride through
IIDGs	Inverter interfaced distributed generators
RTDS	Real time digital simulator
CC	Central control
P, Q	Active and reactive power of the DG
I_d^+, I_d^-	Positive and negative sequence DG current (d component)
V_k^+, V_k^-	Positive and negative sequence voltage at bus k.
V_j^-, V_l^-	Negative sequence voltage at adjacent buses (j, l) to bus k
v_{p1}, v_{p2}	Voltage at point $p1$ and $p2$
$f1, f2$	Objective functions
n	Number of buses
I_{abc}^{limit}	DG current limit
$Q_{\max}$, Q_{ref}	Maximum and reference reactive power
V_a^+, V_b^+, V_c^+	Positive sequence phase a, b, c voltages
Y_{jk}^-	Negative sequence admittance between buses j and k
$I_{d\_\text{ref}}^+$, $I_{q\_\text{ref}}^+$	Positive sequence DG current references (d and q components)
Y_{Gk}^-	Negative sequence admittance of DG connected to bus k
VUF^{lmt}	VUF limit
$I_{Gd}^-, I_{Gq}^-, I_{G0}^-$	Negative sequence d, q and 0 components of DG

✉ Yadala Pavankumar
pavankumaryadala008@gmail.com

1 Department of Electrical Engineering, Jadavpur University, Kolkata, India

V^+, V^-, V_{nom}	Positive sequence, negative sequence and nominal voltage
I_k^-	Negative sequence current at bus k
F	Overall objective function
$w1, w2$	Weight coefficients
N, D	Population size and problem dimension
I_{abc}^+	Positive sequence component of DG current
V_a^-, V_b^-, V_c^-	Negative sequence phase a, b, c voltages
I_{abc}^-	Negative sequence component of DG current.
V_{Gk}^-	Negative sequence voltage od DG connected to bus k
I_{abc}	DG current

1 Introduction

The usage of the renewable energy sources (RES) as a solution for the global climate changes and energy crisis brings more attention towards the integration of renewable sources into the power network. The microgrids are controllable entities consisting of multiple renewable energy sources, energy storage devices and loads, which can be controlled and operated locally. The power electronic interfaces are used to connect the RES to the microgrid, which makes the IIDG control more flexible in non-ideal conditions [1]. The voltage and current signals of the converter can be controlled by controlling the positive, negative and zero sequence quantities in dq reference frame to tackle different issues within the microgrid [2]. The power quality issues often become very critical in the microgrids and the voltage unbalance is one of the most severe issues which may lead to the violation of the grid standards [3]. There are different reasons for voltage unbalance in the microgrid viz. faults, unmatched transformer impedance and the most common one is the presence of single phase loads and unbalanced loads [4]. Moreover, the IIDG control systems are often exposed to voltage sags.

Due to voltage sags, IIDG control systems may experience disturbance which may hamper the continuous and safe operation of power distribution network [5]. Moreover, the operation of the sensitive loads may be disrupted. Therefore, IIDGs should have voltage support abilities and low voltage ride through (LVRT) capability for operation in non-ideal conditions [6, 7]. In non-ideal conditions, the DG may produce high amount of current which may cause damage to the semiconductor devices present in the IIDGs and also there may be sudden loss in the active power injection. To handle these issues viz. voltage support, unbalance compensation, active power control and current limitations, the IIDG control systems should be flexible and should be able to respond quickly as per requirement.

In recent times the researchers proposed different techniques for the DG control during unbalanced conditions. The authors in [8] presented an analytical study on different control strategies to reduce the oscillations in the active and reactive power as well as in the DG phase currents. Ref. [9] proposed flexible control strategy based on the reference current generator to reduce the oscillations in the active and reactive power outputs of the DG and is focussed to limit the over current injection by the DG. Ref. [10] proposed a control technique which can deliver constant amount of reactive power from the DG to support the PCC voltage. The main drawback of this control technique is that voltage is not supported effectively and also it is difficult to select a proper power reference which may result in overcurrent scenario. To overcome this drawback, LVRT strategy has been incorporated by which the DGs inject the required amount of reactive current to mitigate the voltage drop. The authors in [11] proposed an advanced voltage support scheme for the DGs interfaced through the converters. The proposed method utilised the zero sequence components to overcome the drawbacks in the traditional voltage support schemes. The symmetric sequence based voltage support scheme has been proposed in [12], where the regulators are designed based on the symmetrical components to support the voltage dip in the system. The proposed method consists of three different current controllers and also linear quadratic regulator to satisfy the LVRT requirements. The wrong selection of the controller may lead to undesired performance of the system. Ref [13] introduced asymmetrical ride through control in which the control strategy enforces the DGs to properly regulate the voltage and the control technique determines the references for the current from the symmetric voltage components. Based on the positive sequence and negative sequence susceptance and conductance, the authors in [14] proposed a control scheme utilising the instantaneous active power theory, but it only focussed to compensate the short term voltage sags. Ref. [15] proposed a current control scheme for three phase voltage source inverter to mitigate the voltage sags in the grid connected photovoltaic-based power plants. The main drawback of this scheme is that it requires separate control for each phase of the voltage source inverter. A novel control strategy for the converter is developed in [16] to compensate the voltage dips based on balanced positive sequence current control and instantaneous active power control, but the control strategy is more focussed to reduce the fluctuations in the active power. In Ref. [17] a control strategy is developed for the three phase grid connected inverter to enhance the positive sequence voltage and also to reduce the negative sequence voltage under non ideal conditions. However, these methods depend highly on the system parameters and X/R ratio.

In recent times some researchers put efforts on the unbalance voltage compensation. In [18] the authors proposed a proportional resonant controller in complex form using communication link to mitigate the voltage unbalance. The proposed technique shares the compensation burden with each DG. Ref [19] proposed a multiple agent system in multi-microgrids for voltage regulation in which the agents collect data from each microgrid and communicate within the microgrids. To implement this method, large amount of data is required to be collected and it is prone to malfunction due to any communication failure. Based on the state space analysis, a dynamic phasor method is proposed for the microgrid consisting of multiple IIDGs [20]. The authors in ref [21] proposed an optimisation based voltage unbalance compensation for multi-bus microgrid, but there is no provision for giving priority to voltage support. Lagrange multiplier has been utilised in [22] to reduce the load bus negative sequence voltage so as to maximise the voltage support. Ref [23] introduced a new control strategy for grid tied IIDG but it is mainly focussed to support the voltage by supplying the maximum amount of reactive power. An imbalance voltage mitigation technique based on the minimum current control for the IIDGs is introduced in [24], in which the authors have considered multi-objective control to handle different issues. Ref. [25] introduced a novel control technique for the parallel operated grid connected inverters in the microgrid, in which the control strategy focussed to reduce the oscillations in the active and reactive power outputs of the DGs, inject the reactive power to support the positive sequence voltage and also to avoid the over current limitation of the DG. But the proposed scheme is not able to prioritise specific compensation depending on the requirement.

From the existing literature survey it has been observed that voltage unbalance is a major power quality issue in electrical distribution network which adversely affects the connected load and other equipment connected to the network. The main cause of voltage unbalance is the connection of single phase loads and the integration of small scale distributed generations in three phase networks. It can also happen when faults occur on the generation side or due to unmatched impedance of the transformers. Many recent literature addressed the voltage unbalance issue considering the current limit of the inverters but there is a need to consider multiple objectives such as voltage support, unbalance compensation, current limitation and active power control. The control objectives have to be considered simultaneously for better operation of the IIDGs in the microgrid. Hence, this study presents a new optimization based two stage multi-objective control strategy for the microgrid which simultaneously addresses several issues. It always injects maximum possible active power and voltage unbalance has been mitigated with simultaneous active power management and maximum possible positive sequence voltage support. The two stage control viz. local control and central control effectively monitor and addresses the issues related to voltage unbalance, positive sequence voltage support and active power curtailment. The developed technique enables correction of voltage profile and voltage unbalance, satisfying customized requirement of the consumers at different buses abiding the current limitation. The contributions of the proposed approach can be summarised as follows:

- A two stage flexible multi-objective control strategy has been developed for the microgrid consisting of different IIDGs. The control strategy operates locally and also centrally. The local control works individually for each DG and coordinates with the central control to deliver the optimised references for each IIDG.
- The positive sequence voltage at the terminals of the DGs has been supported as much as possible by supplying the required amount of reactive power.
- The voltage unbalance factor (VUF) at the load buses has been reduced as much as possible by supplying the negative sequence quantities from the DGs maintaining DG currents within the safety limits.
- Unlike other conventional techniques, the proposed control strategy is able to inject the maximum amount of active power during the compensation.
- The injection of positive and negative sequence quantities from the DGs can be suitably prioritised depending upon the severity of the voltage unbalance and voltage sag which has not been addressed in other voltage unbalance compensation schemes.
- The proposed approach is tested for diverse conditions including grid imbalance.

This article has been organised into six sections. In Sect. 2 different control objectives of this study have been explained and also the problem statement and optimization algorithm have been discussed. The proposed two level control strategy (local control and central control) of the IIDG is explained in Sect. 3. Section 4 presents the simulation results of the proposed approach under different operating conditions through case studies. The proposed approach has been compared with similar approaches from the recent literature to explain the superiority of the proposed approach in Sect. 5. Finally the conclusion of this work has been presented in Sect. 6.

2 Problem formulation and control objectives

The presence of single phase loads as well as unbalanced loads causes several detrimental issues in the microgrids. Voltage unbalance is one of the major issues that occur due to these unbalance loads. Moreover, the voltage quality becomes vulnerable at the load buses because of the reduction in the positive sequence voltage. The DGs are connected to the microgrid via power electronic interfaces which necessitate flexible microgrid operation by properly controlling the DGs. The studies revealed that while compensating these issues, the DGs present in the microgrid start to inject more current and it may be possible that the overall DG output current may exceed safety limit. Moreover, it creates uncertainty in the active power management. To overcome all these issues, this study aims to supply the positive sequence quantities in order to support the positive sequence voltage, minimise the unbalance voltage compensation through supply of negative sequence quantities and also ensuring the DG overall current under the safety limit with proper active power control. The control objectives of this study are explained in the following subsections.

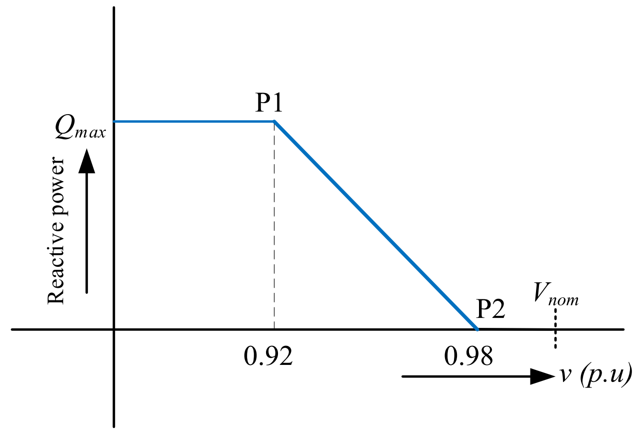

Fig. 1 Reactive power requirement to support the positive sequence voltage

2.1 Active power control

During voltage sags there is always a risk of sudden active power drop. To mitigate that and to use the full DG capacity, the control strategy in the proposed method is designed in such a way that the DG delivers the maximum allowable active power to the grid. The average active power output of the DG can be expressed in *dq* domain as given in Eq. (1) [23].

$$P = I_d^+ V^+ + I_d^- V^- \tag{1}$$

where, V^+ and V^- are the positive and negative sequence voltages. In this work, for simplicity the active power of the DG is injected through positive sequence current I_d^+ and I_d^- is zero. Therefore, from Eq. (1) the reference value for I_d^+ can be obtained from Eq. (2) with the known value of active power output (P) [23].

$$I_{d\_ref}^+ = \frac{P}{V+} \tag{2}$$

The current reference obtained from Eq. (2) is the initial reference which injects the maximum amount of active power in the microgrid. The current reference ($I_{d\_ref}^+$) can be updated depending on the DG current limitation.

2.2 Positive sequence voltage support

To maintain voltage stability during non-ideal conditions, the positive sequence voltage has to be maintained near to the nominal voltage. The conventional methods may not be able to fully support the positive sequence voltage. Therefore, in this work the reactive power has been supplied by the DGs as much as possible to support the positive sequence voltage. The reactive power supplied from the DG according to voltage drop is given in Fig. 1. The reactive power reference has been calculated initially from Eq. (3), from which the q component of the positive sequence current reference ($I_{q\_ref}^+$) is obtained.

$$Q_{\text{ref}} = \begin{cases} Q_{\max} & if\ v \le v_{p1} \\ Q_{\max} + \frac{Q_{p2} - Q_{\max}}{v_{p2} - v_{p1}}(v - v_{p1}) & if\ v_{p1} < v < v_{p2} \\ 0 & if\ v_{p2} < v < v_{\text{nom}} \end{cases} \tag{3}$$

where v_{p1} is the voltage at P_1, v_{p2} is the voltage at P_2 and v_{nom} is the nominal voltage.

When the positive sequence voltage drops below 0.92 p.u, the DG delivers the reactive power at full capacity. When it is above 0.98 p.u., there is no reactive power support from the DG and when the positive sequence voltage is between the 0.92 p.u and 0.98 p.u., the reactive power reference is calculated from Eq. (3).

2.3 Unbalance voltage compensation

The negative sequence current consumed by the unbalanced loads connected to load buses, flows through the line admittance and causes the load buses to experience voltage distortion. Due to the voltage distortion, the voltage quality deteriorates causing problems to the electrical equipment which are sensitive to the voltage quality. If the DGs are able to deliver the negative sequence quantities, the voltage unbalance at the load buses can be compensated. Therefore, by supplying the proper amount of negative sequence quantities from the DGs, the load bus negative sequence voltage can be regulated. This requires the power flow to be calculated. A benchmark low voltage microgrid network [21] as shown in Fig. 2 has been considered to demonstrate the compensation scheme. The load flow has to be calculated for this purpose and the negative sequence equivalent network for

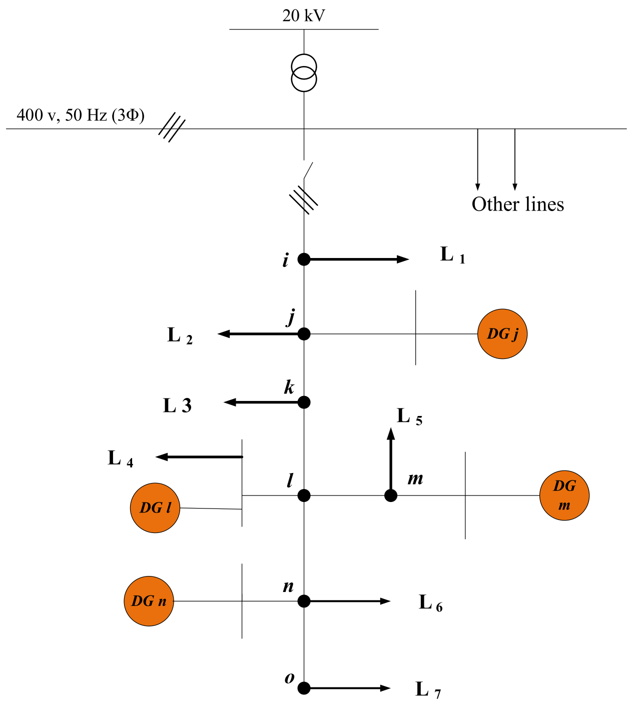

Fig. 2 Microgrid test system

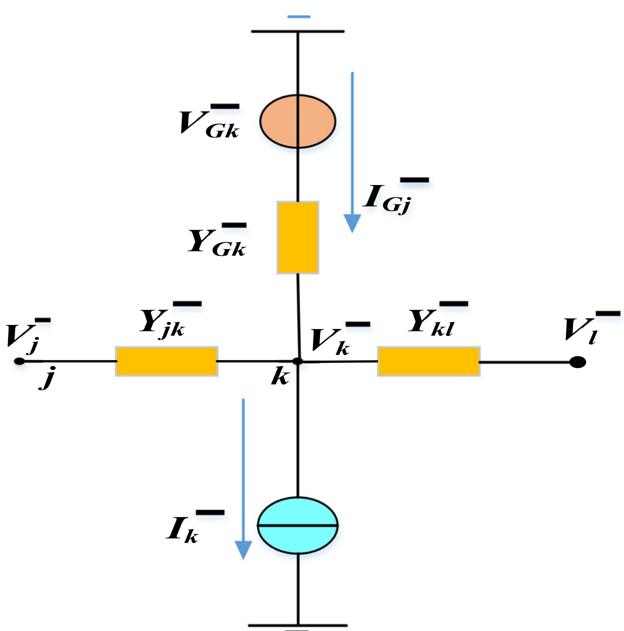

Fig. 3 Negative sequence equivalent of bus k

the considered test system is required. The simplified negative sequence equivalent network at bus k is shown in Fig. 3 in which it is assumed that bus k is a DG connected bus. From Fig. 3 by using the nodal analysis, the expression for the negative sequence current at node k can be expressed as shown in Eq. (4) [21].

$$I_k^- - Y_{jk}^-(V_j^- - V_k^-) - Y_{kl}^-(V_l^- - V_k^-) + (V_{Gk}^- - V_k^-)Y_{Gk}^- \tag{4}$$

where $I_k^- = i_k^{d-} + ji_k^{q-}$.

Equation (4) can be generalised and rewritten as Eq. (5) [21].

$$V_{Gk}^- Y_{Gk}^- - I_k^- = V_k^-(Y_{Gk}^- + \sum_{k=1}^{n} Y_{jk}^-) - \sum_{\substack{j=1 \\ j\neq k}}^{n} V_j^- Y_{jk}^- \tag{5}$$

where, n indicates the number of buses.

When there is no DG connected to bus k, V_{Gk}^- and Y_{Gk}^- become zero. Based on Eq. (5), n number of linear equations can be formulated with n number of unknowns (V_1^-, V_2^-, … V_n^-) for n number of buses. From Eq. (5) it can be observed that the negative sequence DG voltages (V_{G1}^-, V_{G2}^-,….V_{Gn}^-) and negative sequence bus voltages (V_1^-, V_2^-,…V_n^-) are related to each other. Therefore, the negative sequence bus voltage can be controlled by adjusting the DG negative sequence voltage. Hence, by controlling the negative sequence voltage, the VUF at each load bus can be reduced below a certain level so that the voltage quality can be maintained at the load buses. If the positive sequence voltages at the load buses are known, VUF can be calculated from Eq. (6) which has been considered as one objective function.

$$f_1 = \text{VUF} = \sum_{k=1}^{n} \frac{V_k^-}{V_k^+} \times 100 \tag{6}$$

2.4 DG current limitation

To compensate the voltage unbalance, in addition to the positive sequence quantities the DGs in the microgrid will start to supply the negative sequence quantities. It may cause the overall current of the DG to rise above the safety limit of the DG. The studies indicate that the inverter can operate safely till the overall current of DG is 1.2 p.u of the rated current [23]. Since the DG consists of the semiconductor devices, it has to be operated below the safety limit of the DG output current. Therefore, the control technique in this study makes sure that the DG current is less than the safety limit of the DG. The total current injected by the DG into the grid can be calculated from Eq. (7) [9].

$$\overrightarrow{I_{\text{abc}}} = \overrightarrow{I_{\text{abc}}^+} + \overrightarrow{I_{\text{abc}}^-} \tag{7}$$

The positive sequence component of the DG current is the summation of the d and q components as shown in Eqs. (8)

and (9).

$$\overrightarrow{I_{abc}^{+}} = (I_d^{+} + j.I_q^{-}).\,e^{-j.\theta} \tag{8}$$

$$\left|I_{abc}^{+}\right|^2 = (I_d^{+})^2 + (I_q^{+})^2 \tag{9}$$

With the knowledge of the bus voltage, negative sequence DG voltage and line admittance, the negative sequence component of the DG current can be obtained. The negative sequence component of the DG current for the DG connected to the bus k can be determined from Eq. (10) [21].

$$I_{Gk}^{-} = (V_{Gk-}^{-} V_k^{-}).Y_{Gk}^{-} \tag{10}$$

By reverse Park's transformation, the negative sequence component of the current can be obtained from Eq. (11).

$$\overrightarrow{I_{abc}^{-}} = \begin{bmatrix} \cos(-\theta) & -\sin(-\theta) & 1 \\ \cos\left(-\theta - \frac{2\pi}{3}\right) & \sin\left(-\theta - \frac{2\pi}{3}\right) & 1 \\ \sin\left(-\theta - \frac{2\pi}{3}\right) & \sin\left(-\theta + \frac{2\pi}{3}\right) & 1 \end{bmatrix} \cdot \left[I_{Gd}^{-}\, I_{Gq}^{-}\, I_{G0}^{-}\right]^T \tag{11}$$

From Eq. (11) the required amount of the negative sequence component of the DG current can be obtained. But in order to maintain the DG safety limit, it may be possible that the DG is not being able to provide that much amount of the negative sequence current since it is already supplying required amount of positive sequence current Therefore, after delivering the required amount of positive sequence current the available capacity of the DG can be obtained from Eqs. (12–14).

$$I_{abc}^{\mathrm{limit}^2} \geq \left|\overrightarrow{I_{abc}}\right|^2 \tag{12}$$

$$\left|I_{abc}^{+}\right|^2 + \left|I_{abc}^{-}\right|^2 \leq I_{abc}^{\mathrm{limit}^2} \tag{13}$$

$$\left|I_{abc}^{-}\right|^2 \leq I_{abc}^{\mathrm{limit}^2} - \left|I_{abc}^{+}\right|^2 \tag{14}$$

Equation (14) gives the allowable amount of the negative sequence component of the DG current at which the DG operates safely. Hence, Eq. (14) determines the limit for the negative sequence DG current. Therefore, the DG negative sequence current obtained from Eq. (11) has to be less than or equal to the allowable limit. To achieve this, in this study another objective function as shown in Eq. (15) has been formulated.

$$f_2 = \left|I_{abc}^{-}\right|^2 - \left|I_{abc\_\ available}^{-}\right|^2 \tag{15}$$

To solve the objective functions shown in Eqs. (6) and (15), an optimization approach is required. To minimise the VUF and DG phase currents, optimised references are essential for the DGs to properly supply the compensating quantities. Hence, the optimization problem corresponding to f_1 and f_2 can be developed considering the weight coefficients as shown in Eq. (16).

$$f = w_1 * f_1 + w_2 * f_2 \tag{16}$$

where, w_1 and w_2 are the weight functions, w_2 has been given higher priority so that the output phase currents of the DG always stay well within the desired safety limit. The overall optimization problem can be given as shown in Eq. (17). The optimization algorithm will give the optimised values of negative sequence DG voltages to minimise the VUF along with the optimised positive sequence DG reference currents.

$$F = \begin{cases} \mathrm{Minimise}(f) \\ \mathrm{VUF} < \mathrm{VUF}^{\mathrm{lmt}} \end{cases} \tag{17}$$

2.5 Artificial cooperative search algorithm

To solve the optimization problem stated in Eq. (17), Artificial cooperative search (ACS) algorithm has been used in this study. The behaviour of the natural species like butterflies, honey bees and bird species is the inspiration behind the development of the ACS algorithm. The steps involved in the optimization algorithm are given below:

Step 1 Initialising the population, decision variables and its boundary limits. In ACS algorithm two superorganisms (A, B) are initialised randomly using Eq. (18). Each superorganism A and B, consists of sub-superorganisms.

$$\begin{aligned} A_{(i,j)} &= \mathrm{Low}_j + \mathrm{Rnd.}(\mathrm{Up}_j - \mathrm{Low}_j) \\ B_{(i,j)} &= \mathrm{Low}_j + \mathrm{Rnd.}(Up_j - \mathrm{Low}_j) \end{aligned} \tag{18}$$

where, $i = 1,2,\ldots.N$ and $j = 1,2,\ldots.D$

The objective function is defined as.

Minimise $f(x)$,

where, x is subjected to $x_{i\mathrm{low}} \leq xi \leq x_{i\mathrm{up}}$ $(i = 1,2,\ldots.D)$. For each sub superorganism of A and B the fitness $(f(x))$ will be evaluated.

Step 2 The superorganisms consist of sub-superorganisms (random population) migrating to the productive feeding areas. In that process, the superorganisms A and B detect the predator and prey using two random variables. When Rnd1 < Rand2, the predator will be initialised with superorganism A and with a key value 1. Here, Rnd1 and Rnd2 are random variables. If Rand1 > Rand2, then the predator will be initialised with superorganism B and with the key value 2. Similarly, the prey will be initialised.

Step 3 The superorganisms try to find the global minimum and in that process both the superorganisms cooperate with each other to interact biologically. The organisms, which interacted biologically are called active individuals and the biological interaction depends on the scale factor (R). After biological interactions, the new superorganism will be formed as expressed in Eq. (19).

$$x_{(i,j)} = \text{predator}_{(i,j)} + R.(\text{prey}_{(i,j)} - \text{predator}_{(i,j)}) \quad (19)$$

Step 4: The fitness will be calculated for each sub-superorganism of the new superorganism (x) and it will be compared with the fitness of the sub superorganism of the predators. If the fitness of the sub superorganism of x is better than the predator, the predator sub-superorganism will be updated. Finally, the predator gets updated and it will be initialised into A or B depending on the key values assigned earlier.

Step 5 Repeat steps 2–5 until the optimization problem converges or up to the maximum number of iterations.

DG negative sequence voltages (V_{G1}^{-}, V_{G2}^{-},....V_{Gn}^{-}) are considered as design variables and VUF as constraint. The optimization algorithm takes the IIDG data and load bus data and converges the optimization problem (objective function). Finally, it sends the optimised references to each DG.

3 Proposed multi-objective control strategy

To achieve the control objectives as mentioned in the above section, the multi-objective control strategy has been implemented in this study. The control strategy is aimed to supply the reactive power through the positive sequence quantities in order to support the positive sequence voltage and secondly it is aimed to minimise the voltage unbalance as much as possible by injecting the negative sequence quantities with efficient balance between the active power production and current limitation. To implement these objectives simultaneously in the microgrid test system consisting of several DGs, the proposed control strategy has been developed in two stages viz. local control and central control where the central control coordinates with the local control.

3.1 Local control

The microgrid test system consists of different IIDGs connected at different buses viz. DG_j, DG_m, DG_l and DG_n. The local control is the control which controls the DGs individually. The main task of the local control is to monitor each DG individually, track and control the positive sequence DG currents (I_d^+,I_q^+) locally and update it after getting feedback from the central control. Secondly, it will receive the references for the reactive power support (Q_{ref}) and active power production ($I_{d\_\text{ref}}^+$) from the central control and track the d and q components (I_d^+,I_q^+) of the positive sequence current which will be fed to the grid side inverter.

3.2 Central control

The central control (CC) operates globally in the microgrid and it coordinates with all the DGs. The central control tracks the positive sequence bus voltages (V_1^+, V_2^+, ...V_n^+), negative sequence load currents at each bus (I_1^-, I_2^-, ...I_n^-) and the DG positive sequence currents. Initially, the CC detects the voltage sag and depending on the voltage sag, the CC classifies the scenario. In this study two scenario classifications are considered, which are (1) Active power prioritisation during small voltage sag at the PCC. In this scenario, the first priority is given to the active power production of the DG and the DG will get the reference current to deliver the maximum active power. The next priority has been given to the positive sequence voltage support and finally remaining capacity of the DG, if any, is utilised for unbalance voltage compensation. (2) Positive sequence voltage support prioritisation during large voltage sag at the PCC. In this scenario, the first priority is to provide the reactive power to support the voltage magnitude. The DG starts to supply the maximum amount of the reactive power, then the unbalance compensation is prioritised and finally the remaining capacity is used for the active power injection.

3.3 Application of the proposed multi-objective control strategy

Initially the control system detects the voltage sag and the scenario classification is performed depending on the positive sequence voltage. The control strategy follows the following steps:

Step 1 For scenario 1: The active power injection of the DG is prioritised in this scenario. Therefore, the initial reference current for active power ($I_{d\_\text{ref}}^+$) which injects the maximum amount of active power into the grid will remain same. Then to support the positive sequence voltage, the required reactive power from each DG will be calculated depending on the voltage level as given in Eq. (3). These references are initially fed to the local control and it tracks I_d^+ and I_q^+ values. Then the optimization problem which is mentioned in Eq. (17) is solved using the (ACS) algorithm.

For scenario 2: In this scenario, since the voltage sag is more, the DGs prioritise to deliver the full capacity of reactive power and therefore, the initial $I_{d\_\text{ref}}^+$ will be fed into the control system. In this scenario, it is assumed that the second priority is given to the voltage unbalance compensation. To achieve that, voltage unbalance constraint has been included in the optimization problem as given in Eq. (19). Here, the DG is delivering maximum amount of reactive power, providing

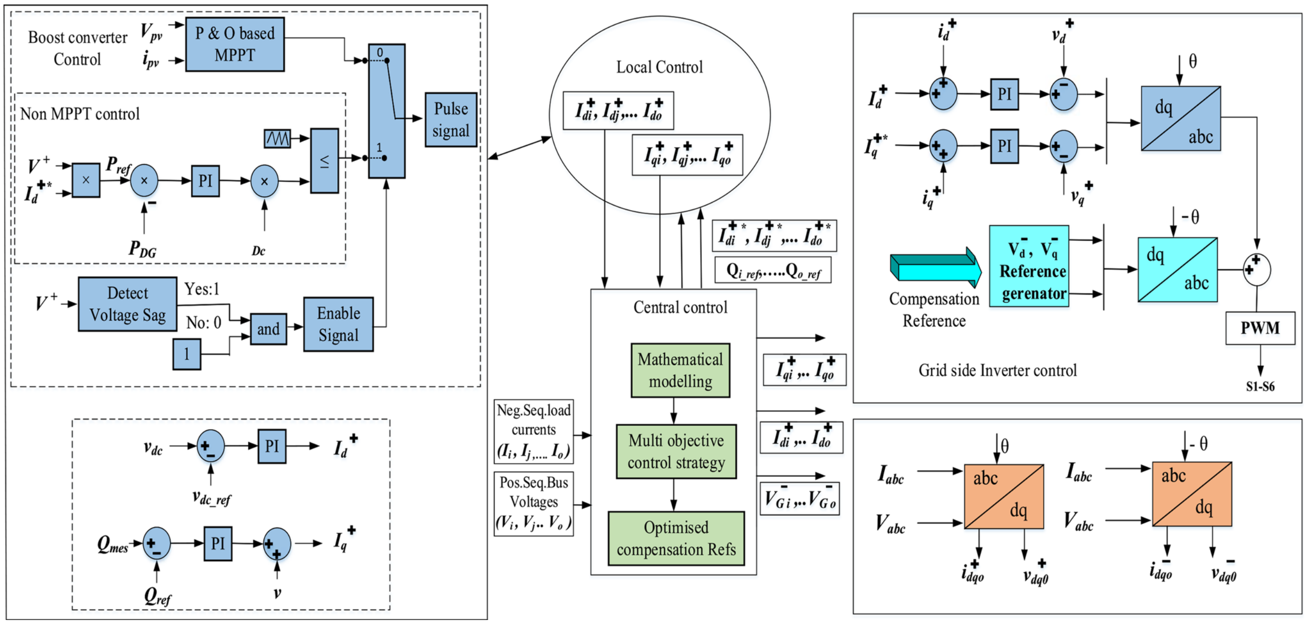

Fig. 4 Overall control structure of the proposed scheme

unbalance compensation in addition to the active power production. Therefore, it may be possible that the DG overall current will exceed its limit. In this case, the control technique has to sacrifice the active power production so that the DG can accomplish other objectives. For this, the active power current reference ($I_{d\_ref}^{+}$) will be updated accordingly following Eq. (20).

$$Q_{\text{ref}} = Q_{\max} \tag{20}$$

$$\text{VUF} \leq \text{VUF}^{\text{lmt}} \tag{21}$$

$$I_{d\_ref}^{+} = I_{d\_ref}^{+} \pm \Delta I_{d}^{+} \tag{22}$$

where, ΔI_{d}^{+} is considered as 10% of the initial current reference and the optimization algorithm will update $I_{d\_ref}^{+}$ which results in active power curtailment until the DG currents reach the safety limits. The positive sign is considered during the restoration of the active power and the negative sign is considered during active power curtailment.

Step 2 Next the optimised values of the positive sequence DG current references and DG negative sequence voltage references are fed to the DG inverter control as shown in Fig. 4.

Step 3 Finally, the voltage reference signal which is a combination of positive and negative sequence voltages as shown in Eq. (21) is fed to the power converter with the help of PWM.

$$\begin{bmatrix} V_a \\ V_b \\ V_c \end{bmatrix} = \begin{bmatrix} V_a^{+} \\ V_b^{+} \\ V_c^{+} \end{bmatrix} + \begin{bmatrix} V_a^{-} \\ V_b^{-} \\ V_c^{-} \end{bmatrix} \tag{23}$$

4 Simulation results

To evaluate the performance of the proposed flexible multi-objective control strategy, the simulation is carried out for the test model shown in Fig. 2 in MATLAB/ Simulink environment. The three phase three wire low voltage test system have four DGs which are connected *at j, m, l* and *n* buses and seven three phase loads. The rated capacities of the DGs that are connected to the buses *j, m, n* and *o* are 10 kW, 10 kW, 3 kW and 5 kW respectively. The power electronic interfaces (i.e. three phase three leg inverters) are utilised to connect all the DGs to the microgrid. The rated voltage of the test system is considered as 400 V and the frequency is 50 Hz. The DG tie line admittances, feeder tie line admittances and the delta connected three phase loads at each load bus are given in Table 1. To create unbalance, several single phase loads are connected in the microgrid at different time intervals. The population size is considered as 50 and it is observed that the average computational time of solving optimization objective is 0.17 s (converged within 50 iterations). The optimization algorithm runs for every 0.2 s and the obtained optimal references are given to each DG, which guarantees safe convergence in each run. A low-bandwidth

Table 1 Feeder line data and three phase load data

Tie lines	Conductance (S)	Susceptance (S)	Bus	Load (Ω)
Between *i* & *j*	0.1269	0.6379	*i*	588.2
Between *j* & *k*	0.3032	1.7148	*j*	1425.6
Between *k* & *l*	0.4683	3.9230	*k*	588.2
Between *l* & *m*	0.0332	1.7148	*l*	588.2
Between *l* & *n*	0.3032	1.7148	*m*	588.2
Between *n* & *o*	0.3032	1.7148	*n*	588.2
DG's	0.3032	1.7148	*o*	588.2

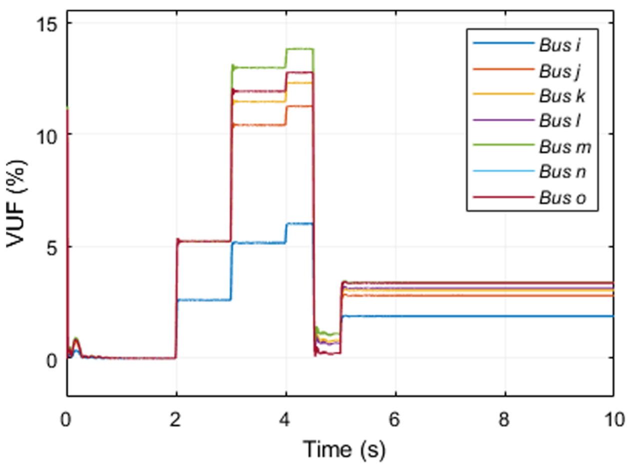

Fig. 5 VUF at each load bus in case 1

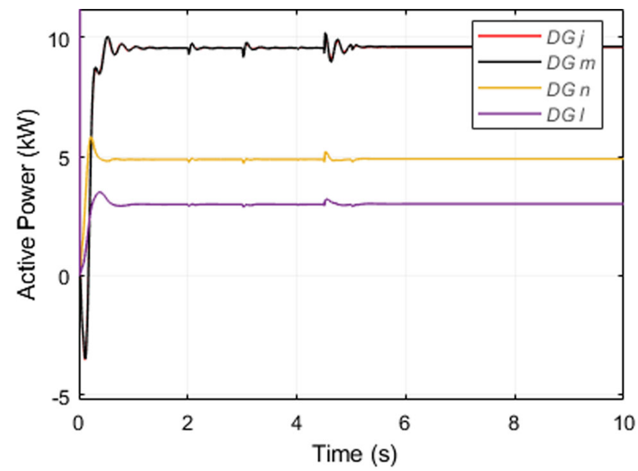

Fig. 6 Active power output of the DGs in case 1

communication link is capable enough to perform the management of the whole task. Different case studies are carried out to evaluate the robustness of the proposed control strategy.

4.1 Case 1

4.1.1 During small voltage sag

The performance of the proposed method is assessed during small voltage sag in this case study. In addition to the balanced delta connected three phase loads, the single phase loads are connected at different buses. The single phase loads (50Ω, 45Ω and 143Ω) are connected to the two phases of the three phase balanced loads at the load buses *j, m* and *i* at 2 s, 3 s and 4 s. All the DGs in the microgrid are producing maximum active power and the load buses experience increment in the negative sequence voltage because of the presence of the single phase loads which makes the VUF to rise at each load bus as shown in Fig. 5. Moreover, the positive sequence voltage at the DG terminals are also reduced due to the extra burden of the single phase loads. The positive sequence voltage at the terminals of DG_j, DG_m, DG_l and DG_n after 4 s is observed as 0.978 p.u, 0.976 p.u, 0.973 p.u and 0.974 p.u

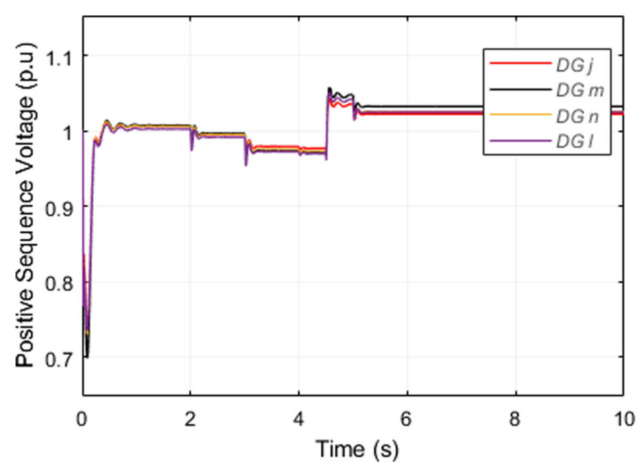

Fig. 7 Positive sequence voltages at the terminals of the DGs in case 1

respectively. At 4.5 s the control strategy is started and the positive sequence voltages at all the DG terminals are above 0.92 p.u. Therefore, the control strategy works in scenario 1 mode. Figure 6 illustrates that even after 4.5 s all the DGs continue to deliver the active power at full capacity. Also, as shown in Fig. 7 and tabulated in Table 3, the positive sequence voltages at the terminals of the DGs rise near to the nominal

Table 2 VUF in different cases

Load buses	Case 1		Case 2			Case 3	Case 4	Case 5
	VUF (%)		VUF (%)			VUF (%)	VUF (%)	VUF (%)
	After 4.5 s	After 5 s	After 5.5 s	After 6.5 s	After 7 s	After 3.5 s	After 4.5 s	After 4.5 s
i	1.1	1.8	5.2	4.7	3.5	6.6	1.7	2.7
j	1.1	2.7	8.5	6.4	4	4.9	2.3	4.4
k	0.8	3.1	9.4	6	3	6.6	2.7	4.9
l	0.7	3.2	9.4	5.5	2.5	7.4	2.8	5
m	1.1	3.4	9.2	4.3	1.6	8.3	4	6.1
n	0.3	3.38	9.2	4.9	2.1	7.6	2.4	4.6
o	0.3	3.38	9.2	4.9	2.1	7.6	2.4	4.6

voltage at each DG, since the DGs are supplying the reactive power. VUF has been reduced at each bus at 4.5 s as shown in Fig. 5, since all the DGs are producing the compensating currents. At 5 s another single phase load of 75 Ω has been added to bus n and all the DGs receive the updated references. The reactive power support has been adjusted as per the new references and the positive sequence voltages at the terminals of the DGs which are connected to the load buses *j, m*, *i and n* are tabulated in Table 3. The reactive power support from each DG is shown in Fig. 8. Here, since the active power is prioritised, the DGs are producing full active power and to maintain the DG phase currents within the safety limits, the control has to sacrifice the voltage unbalance compensation since the DG currents are already operating near to the safety limit as shown in Fig. 9. Therefore, as given in Fig. 5 and Table 2, the VUF has been increased slightly at each load bus after 5 s.

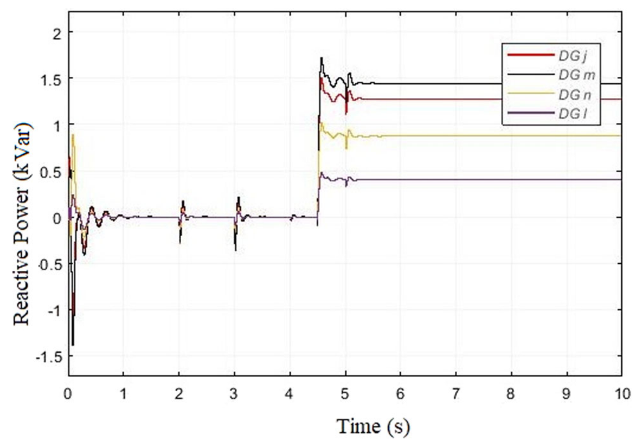

Fig. 8 Reactive power output of the DGs in case 1

Fig. 9 Three phase DG currents in case 1

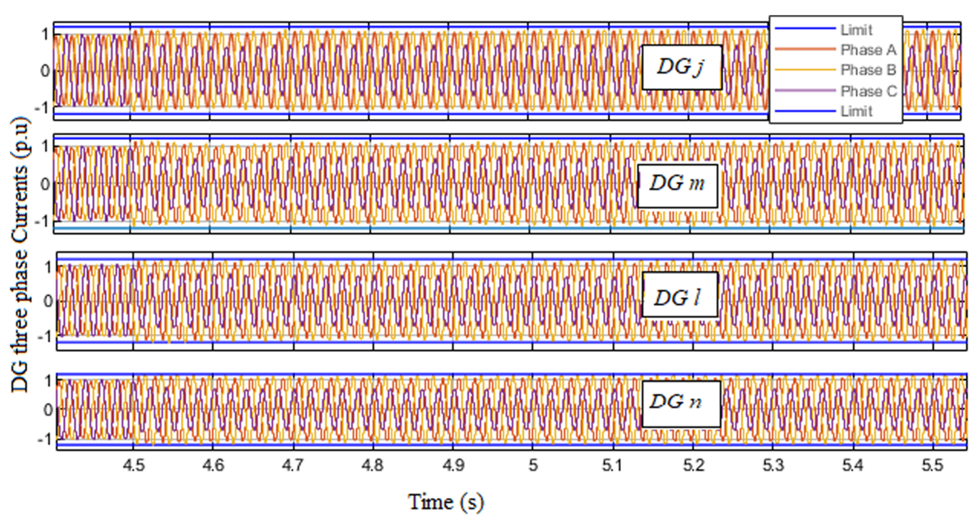

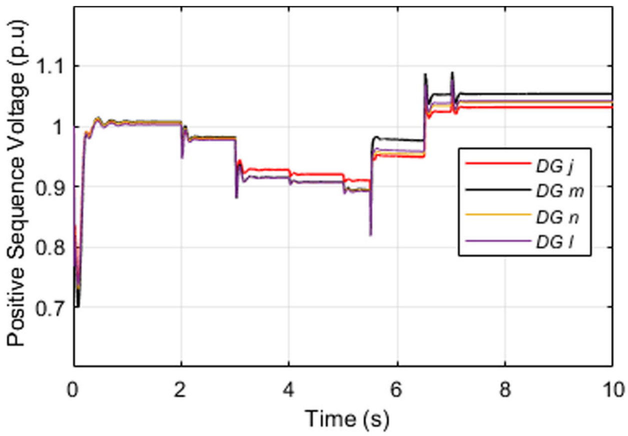

Fig. 10 Positive sequence voltages at the terminals of the DGs in case 2

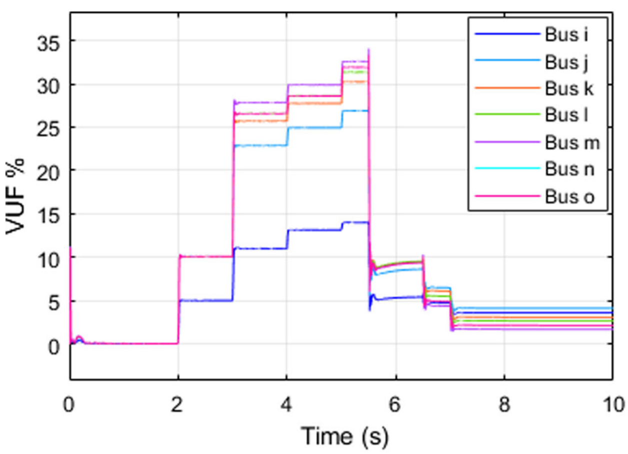

Fig. 11 VUF at each load bus in case 2

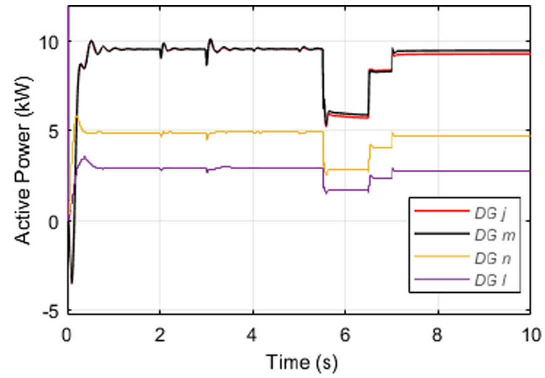

Fig. 12 Active power output of the DGs in case 2

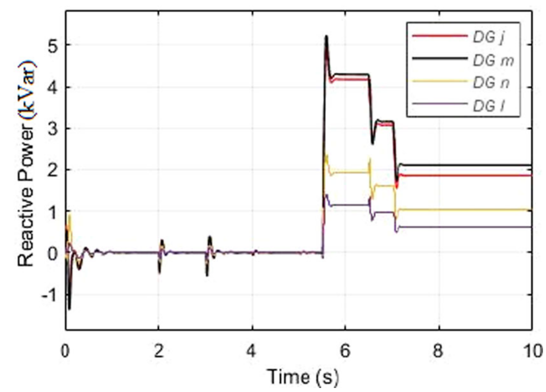

Fig. 13 Reactive power output of the DGs in case 2

4.2 Case 2

4.2.1 During moderate voltage sag

The voltage sag is created in this study by connecting the various single phase loads during different time intervals at different load buses. A 50Ω, 25Ω, 50Ω, 60Ω, 35Ω and 75Ω single phase loads are connected to the load buses *i, j, k, l, m* and *n* respectively between 2 and 5 s. The positive sequence voltages at the terminals of the DGs which are connected to the load buses *j, m, i and n* after 5 s are observed as 0.91 p.u, 0.88 p.u, 0.89 p.u and 0.88 p.u respectively and the maximum unbalance at the load buses has been observed as 32.5%. Here, the PCC voltages of the DGs are less than the 0.92 p.u. and therefore, priority has been given to the supply of the reactive power. The unbalance compensation is prioritised by adding the constraint that VUF at each bus should be less than 10%. The compensation control strategy is started at 5.5 s and all the DGs are injecting the maximum amount of reactive power. Hence, the positive sequence voltages at the DG terminals are raised as tabulated in Table 3 which can also be observed from Fig. 10. Figure 11 shows that the VUF is reduced to below 10% at 5.5 s at all the load buses. Since all the DGs are supplying the reactive power at full capacity and also the majority of the DG capacity is utilised for the unbalance compensation, the DGs had to curtail the production of the active power to maintain the DG phase currents within the limits. From Fig. 12 it is visible that the active power is curtailed at 5.5 s and the reactive power injected by the DGs is shown in Fig. 13. The DG currents are within the safety limit as shown in Fig. 14. To test the robustness of the proposed control strategy, it is assumed that at 6.5 s the single phase loads which are connected to the load buses *m* and *n,* are removed. The central control sends the updated references to each DG and it can be seen that the positive sequence voltages at the terminals of the DGs have been raised above 1 p.u after 6.5 s as shown in Fig. 10. Since two unbalanced loads are removed, the DGs have extra capacity and therefore, the active power injection of the DGs is enhanced after 7 s as shown in Fig. 12. Again, another single phase load at bus *k* is removed at 7 s and the control technique updates the references of the DGs. It can

Table 3 Positive sequence voltages (V^+) at the terminals of the DGs

DGs	Case 1		Case 2			Case 3	Case 4	Case 5
	V^+ (p.u)		V^+ (p.u)			V^+(p.u)	V^+ (p.u)	V^+ (p.u)
	After 4.5 s	After 5 s	After 5.5 s	After 6.5 s	After 7 s	After 3.5 s	After 4.5 s	After 4.5 s
DG_j	1.03	1.021	0.98	1.03	1.031	0.982	1.018	1.017
DG_m	1.045	1.031	0.98	1.05	1.05	1.002	1.014	1.013
DG_n	1.04	1.026	0.965	1.04	1.041	0.994	1.017	1.016
DG_l	1.04	1.025	0.96	1.038	1.039	0.994	1.018	1.017

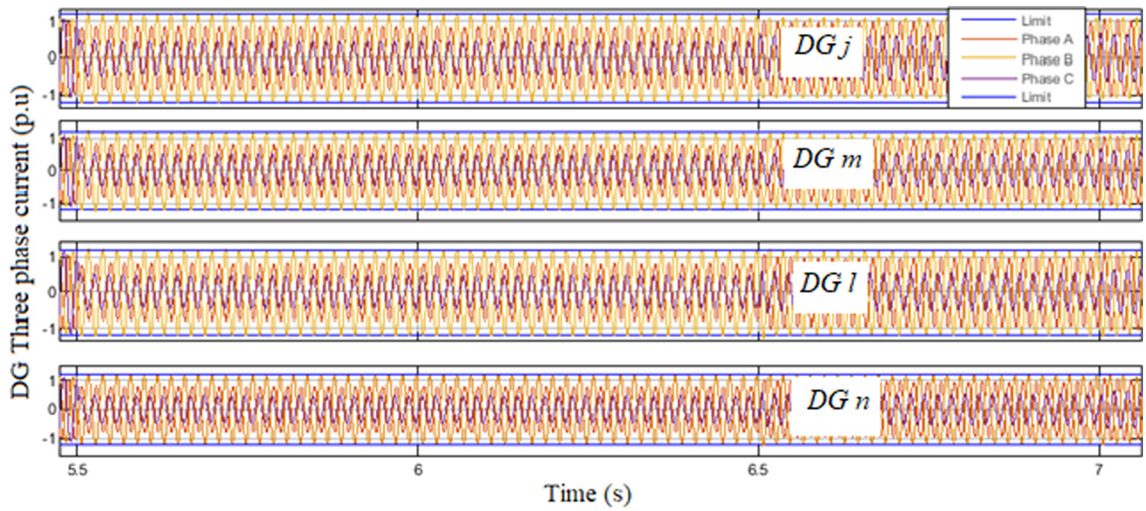

Fig. 14 Three phase DG currents in case 2

be seen from the results that the DGs are able to support the positive sequence voltage and unbalance compensation fully and also the active power injection of the DGs is restored to full capacity. The detailed VUF at each load bus during each step has been tabulated in Table 2. The DG phase currents are shown in Fig. 14 and it can be observed that all the phase currents are well within the safety limit.

4.3 Case 3

4.3.1 Under grid imbalance

The proposed control strategy has been evaluated under grid imbalance to ensure its effectiveness. An unsymmetrical fault has been created at 2 s near to the grid to create the grid imbalance [26] as a result of which VUF at the grid becomes 24% and it is observed that the positive sequence voltage at the DG connected buses are dropped below 0.9 p.u. The control strategy is started at 3.5 s and all the DGs start injecting reactive power. It can be observed from Table 3 that the positive sequence voltage of each DG has been raised to near the nominal voltage. The reactive power sharing of each DG is shown in Fig. 15. Simultaneously, as shown in Fig. 16, the VUF at each load bus is reduced after 3.5 s, when all the DGs start to supply the negative sequence quantities. Since the DGs are prioritised to inject the reactive power at full capacity with unbalance compensation, the active power injection of the DGs has been curtailed as shown in Fig. 17 to operate

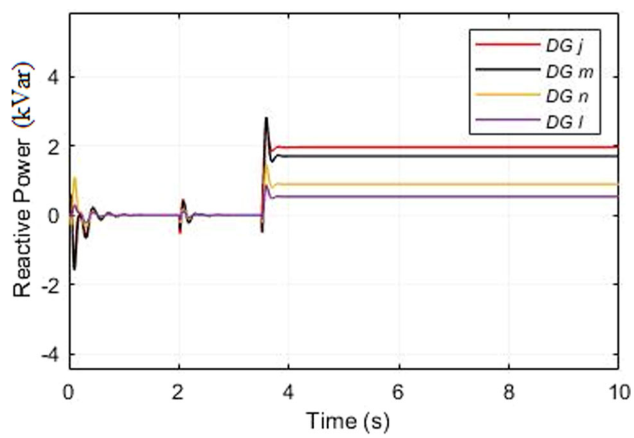

Fig. 15 Reactive power output of the DGs in case 3

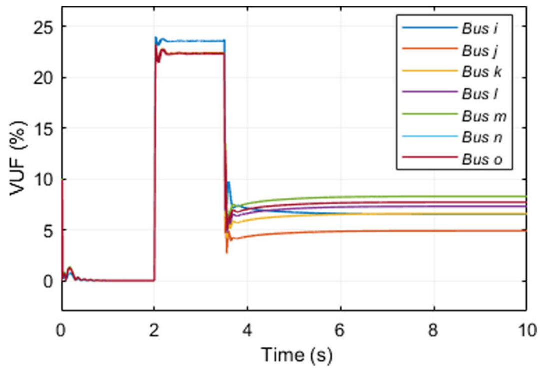

Fig. 16 VUF at each load bus in case 3

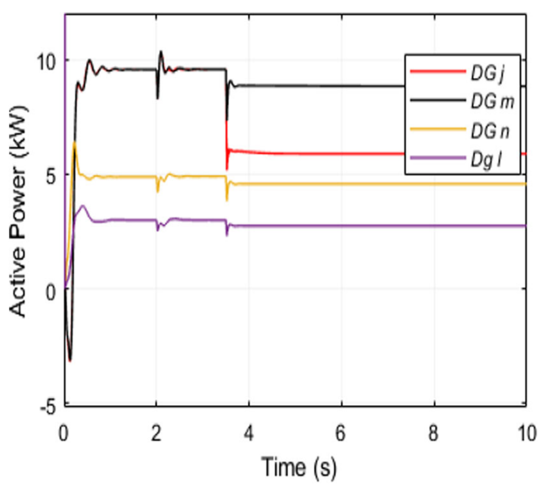

Fig. 17 Active power output of the DGs in case 3

the DG under safety mode. In this case, the fault persists till 10 s. To validate the real time application of the proposed approach, this case study has been implemented in OPAL-RT with RT lab version 19.3.0.228 and RTS OP5600 chassis. The observed grid voltage in DSO from OPAL-RT is shown in Fig. 18, from which it can be observed that due to fault, the grid voltage remains unbalanced till 3.5 s as during this time no compensation is provided and after the DGs start the compensation, the unbalance is reduced. All the phase currents of the DGs are maintained within the safety limit. The positive sequence voltage in DSO under this case study is presented in Fig. 19. The positive sequence voltage is shown in p.u. in Fig. 19. The voltage per division is 0.5 V and the probe multiplier is 1. Therefore, it can be observed from Fig. 19 that the voltage before unbalance is $2 \times 0.5 \times 1 = 1$ p.u.

4.4 Case 4

4.4.1 DG unavailability

In this case study the proposed control strategy is tested under the condition of DG unavailability. It is assumed that DG_m cannot participate in the compensation control. Initially, the central control gets the signal from the local control about the unavailability of the DG and the control system considers the remaining DGs for the compensation control. The loads are considered same as in case 1 till 4 s and at 4.5 s the compensation control has been initiated. From Table 3, it is evident that the positive sequence voltages at terminals of the DGs have been raised near to the nominal voltage. Here, it is noteworthy to mention that even though DG_m is not supplying any reactive power, the positive sequence voltage at this particular bus is also raised near to the nominal voltage since all the other three DGs are supplying sufficient reactive power which affects the voltage at the terminals of DG_m as shown in Fig. 20. Further, the VUF at each load bus is tabulated in Table 2 and also shown in Fig. 21. From Table 2 it is revealed that the VUF at every load bus is slightly higher compared to the VUF in case 1 because in this case the compensation is done only by the three DGs, since only three DGs are available for compensation. All the DGs in this case study are delivering the maximum amount of active power and also it is observed that the compensating DG output currents in all phases are well within the safety limit.

4.5 Case 5

4.5.1 Communication failure

The communication between the local control and the central control plays an important role in the control strategy. It is possible that there might be a communication problem between the local control and the central control and to illustrate this scenario it is assumed that initially all the DGs are available for the compensation control. The central control sends the optimal references to all the four DGs, but due to the communication failure DG_m could not receive the optimal references. The single phase loads are considered as in case 1 till 4 s. At 4.5 s the control strategy started to work. Three DGs participated in the compensation process and one DG only supplied the active power since it did not receive the references. In Table 2 the VUF information at each load bus is tabulated which is also shown in Fig. 22. It can be seen that VUF is more at the load buses compared to case 4 because in this case only three DGs participated in the compensation control, even though the central control sent the references to all the four DGs. The positive sequence voltage at the DG terminals is well supported up to the nominal voltage as shown in the Fig. 23.

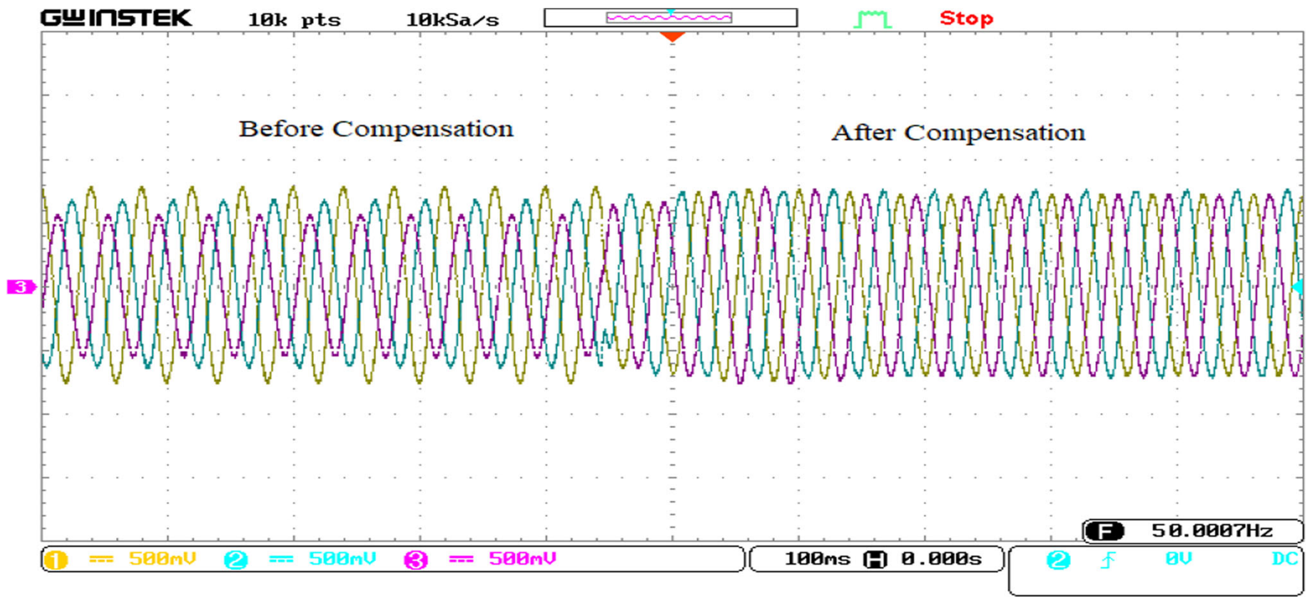

Fig. 18 Three phase grid voltages from RTDS in case 3

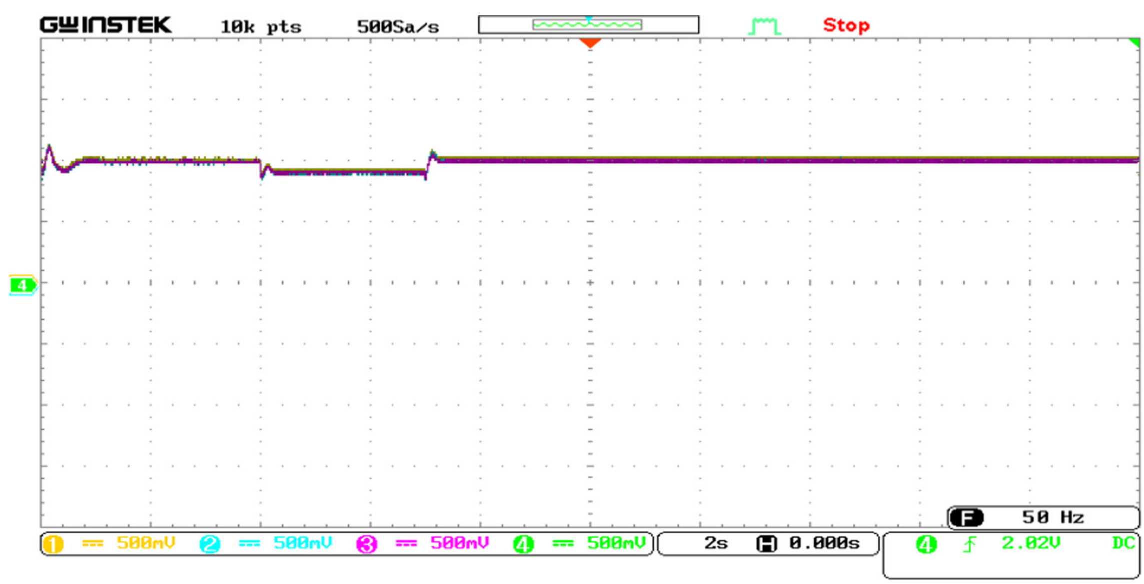

Fig. 19 Positive sequence voltage at the terminals of the DGs in case 3 from RTDS

4.6 Case 6

The proposed control strategy is able to inject the maximum active power into the system even when the DGs are participating in the compensation process. The proposed approach tracks the DG phase currents and allows the DG to inject maximum active power until the DG phase currents reach the safety limit. Therefore, the active power curtailment in the proposed approach is less compared to the conventional approaches, which makes the proposed approach more reliable. To highlight this feature of the proposed approach, an analysis has been carried out for the active power injection by the IIDGs with the active power maximisation (proposed control strategy) and without active power maximisation (conventional control strategy). For this purpose, it is assumed that all the loads are same as in case 2. Here, the PCC voltages of the DGs are less than 0.92 p.u. and therefore, priority has been given to the supply of the reactive power. The compensation control strategy is started at 5.5 s with all DGs injecting the maximum amount of reactive power. Since all the DGs are supplying the reactive power at full capacity and also the majority of the DG capacity is utilised for the unbalance compensation, the DGs had to curtail the production of the active power to maintain the DG

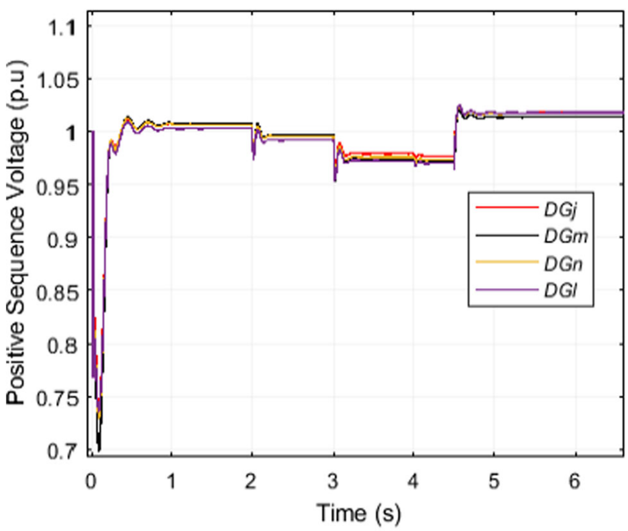

Fig. 20 Positive sequence voltage of DG terminals in case 4

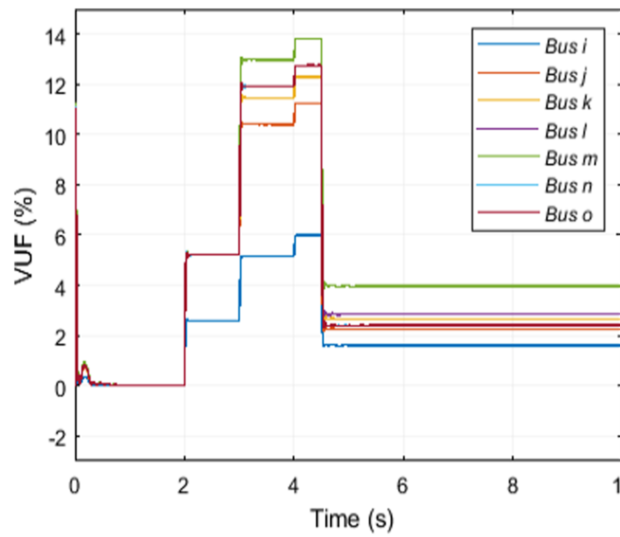

Fig. 22 VUF at each load bus in case 5

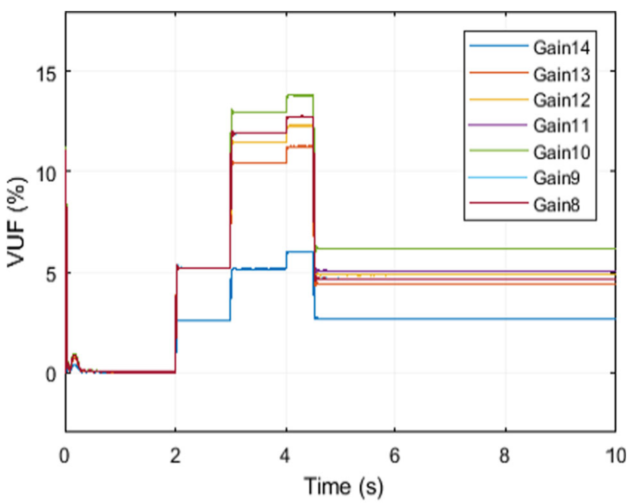

Fig. 21 VUF at each load bus in case 4

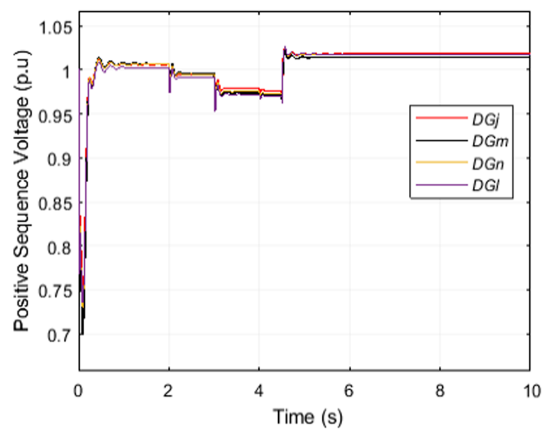

Fig. 23 Positive sequence voltage at the terminals of the DGs in case 5

phase currents within the limits. From Fig. 24 it is visible that the active power is curtailed at 5.5 s. At 6.5 s the single phase loads which are connected to the load buses m and n, are removed and another single phase load at bus k is removed at 7 s. The control technique updates the references of the DGs. It can be seen from Fig. 24 that in the proposed approach, the DGs are able to increase the active power injection, since the compensation burden has been reduced. The DGs curtail the active power injection at 5.5 s to maintain the DG phase currents within the safety limits, but the DGs fail to increase the active power injection after some unbalanced loads are removed in conventional approaches without active power maximisation. Therefore, from this analysis it can be conclude that in the proposed approach, the control scheme can inject maximum amount of active power which makes the system more reliable.

4.7 Case 7

4.7.1 Communication delay

The proposed control strategy requires communication between the local and central control and hence, any communication delay may disturb the performance of the system. The communication delay may happen either from central control to local control or from local control to central control. To illustrate the first scenario, it is assumed that all the loads are considered as same as in case 2 and the central control sends the optimised signals to each DG at 5.5 s, 6.5 s and 7 s. But due to communication delay, DG connected to bus *m* receives the signals delayed by 0.1 s i.e. at 5.6 s, 6.6 s and 7.1 s. It can be seen from Fig. 25a and b, that there is a slight delay in the response of active and reactive power outputs of DG_m. But since the remaining 3 DGs are having no delay, the VUF and positive sequence voltages are maintained well

Fig. 24 Active power injection of IIDGs: **a** DG_j, **b** DG_m, **c** DG_n, **d** DG_l

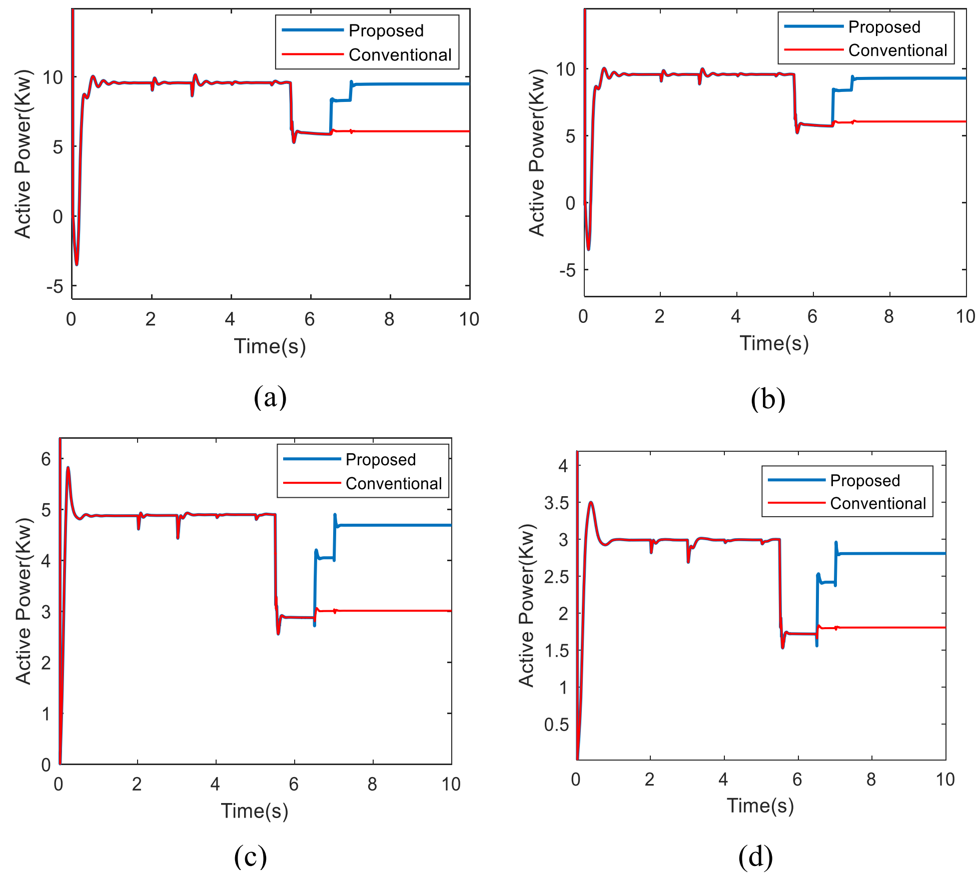

within the required limits as shown in Fig. 25c and d. On the other hand, if communication delay is present from local control to central control, the central control considers the previous data as reference from the local control and executes the optimization algorithm and sends the optimal references. It is noteworthy to mention that, the optimization algorithm runs for every 0.2 s. Therefore, the optimal references will be updated as per requirement after every 0.2 s.

5 Comparative assessment

To highlight the robustness of the proposed approach, comparative study has been conducted with the recently proposed methods in the literature. In this study, a flexible multi-objective control strategy for the IIDG based microgrid is implemented which can support the positive sequence voltage at the DG terminals, provide unbalance voltage compensation and maximise the active power whereas, in [19, 21] and [24] only the unbalance voltage compensation has been considered. Unlike the methods presented in [21] and [22], in the proposed approach, the positive sequence voltage has been supported near to the nominal voltage during voltage sag. In this study, the developed method is able to compensate moderate voltage sags whereas, in [24] only small voltage sags have been mitigated. The methods proposed in [21] and [24] inject constant amount of active power and therefore, these approaches cannot adjust the active power injection depending on the requirement, whereas, the proposed method is able to prioritise and curtail the active power production of the DGs depending on the situation. Moreover, the unbalance compensation control in the proposed method does not depend on the type of the unbalance and it works satisfactorily during grid imbalances, which has not been considered in [19] and [24]. The proposed method only utilises the local data of the measured voltage and current in the control strategy whereas, ref [19] requires the data from multiple agents and from multiple microgrids which increases the chance of malfunction. The communication between the microgrids plays an important role in the control strategy. The failure of communication link, which may cause severe disturbance in the system performance, has not been considered in [19], whereas, the authors in the proposed method investigated the effect of communication link failure on the performance of the algorithm and obtained satisfactory results.

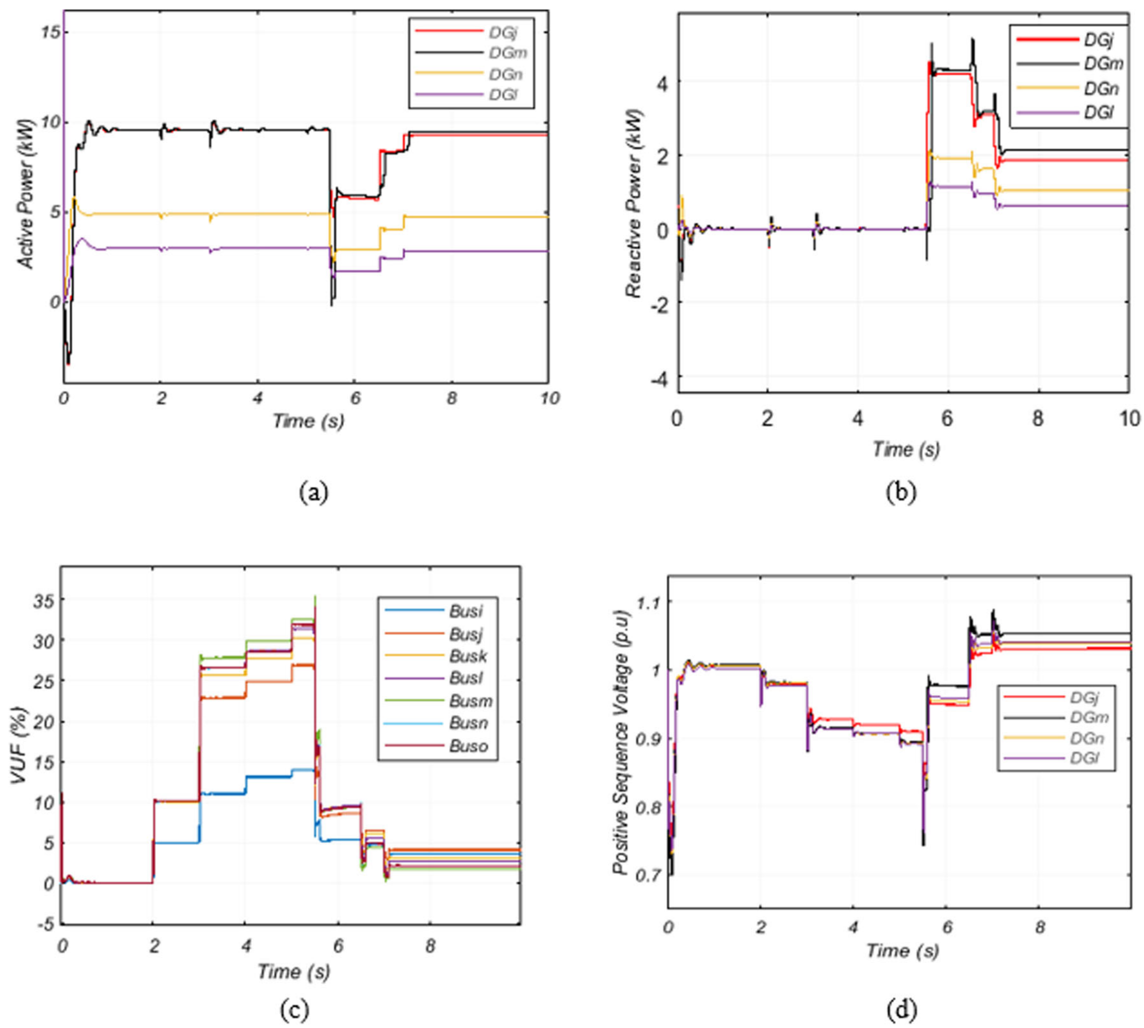

Fig. 25 Results for case 7. **a** Active power output of DGs. **b** Reactive power output of DGs. **c** VUF at the load buses. **d** Positive sequence voltage the terminals of the DGs

6 Conclusion

This work presents a resilient multi-objective control strategy for microgrid to simultaneously support the positive sequence voltage and compensate the voltage unbalance at the load buses. By supplying the reactive power from the DGs, the proposed approach is able to support the positive sequence voltage at all PCC near to the nominal voltage and it is also capable of compensating the voltage unbalance at the load buses as much as possible by supplying negative sequence quantities, maintaining the DG phase currents within the safety limit. Unlike other methods, the control strategy used in this study is able to prioritise the active power injection when the voltage is near to its nominal value and adjusts the negative and positive sequence components to mitigate the voltage sag and voltage unbalance. During small voltage sag, the unbalance compensation can be prioritised and during severe voltage sag the DGs can be prioritised to inject reactive power at full capacity. The grid operator can maintain customized voltage profile at different load buses using this flexible control strategy. The robustness of the proposed technique is tested for grid imbalance and other diverse conditions. The simulation results show that the performance of the proposed approach is satisfactory in the event of any communication link failure or when any DG is not taking part in the compensation process. The test results from the real time digital simulator establish that the scheme is suitable for execution in real time.

Author's contribution All the authors have equal contribution in this article and all the authors reviewed the manuscript.

Funding Not applicable.

Data availability Not applicable.

Declarations

Conflict of interest The authors declare that they have no conflict of interest.

Ethical approval Not applicable.

Consent to participate Not applicable.

Consent for publication Not applicable.

References

1. Member S, Yang G, Member S, Nielsen AH, Member S (2018) A review on grid-connected converter control for short-circuit power provision under. IEEE Trans Power Del 33(2):649–661
2. Merritt NR, Chakraborty C, Bajpai P, Member S (2017) New voltage control strategies for VSC-based DG units in an unbalanced microgrid. IEEE Trans Sustain Energy 8(3):1127–1139
3. Systems P (2012) IEEE standards. IEEE Spectr 12(4):98–98. https://doi.org/10.1109/mspec.1975.6368794
4. Masters CL (2002) Voltage rise: the big issue when connecting embedded generation to long 11 kV overhead lines. Power Eng J 16(1):5–12
5. Stanisavljević AM, Katić VA (2019) Magnitude of voltage sags prediction based on the harmonic footprint for application in DG control system. IEEE Trans Ind Electron 66(11):8902–8912
6. Pavankumar Y, Debnath S, Paul S (2022) Microgrid fault detection technique using phase change of positive sequence current. Int J Model Simul. https://doi.org/10.1080/02286203.2022.2059613
7. Fortmann J et al (2015) Fault-ride-through requirements for wind power plants in the ENTSO-E network code on requirements for generators. IET Renew Power Gener 9(1):18–24
8. Shabestary MM, Mohamed YARI (2016) An analytical method to obtain maximum allowable grid support by using grid-connected converters. IEEE Trans Sustain Energy 7(4):1558–1571
9. Çelík D, Meral ME (2019) A flexible control strategy with overcurrent limitation in distributed generation systems. Int J Electr Power Energy Syst 104:456–471. https://doi.org/10.1016/j.ijepes.2018.06.048
10. Guo X, Liu W, Lu Z (2017) Flexible power regulation and current-limited control of the grid-connected inverter under unbalanced grid voltage faults. IEEE Trans Ind Electron 64(9):7425–7432
11. Shabestary MM, Mohamed YARI (2018) Advanced voltage support and active power flow control in grid-connected converters under unbalanced conditions. IEEE Trans Power Electron 33(2):1855–1864
12. Shabestary MM, Mohamed YARI (2019) Asymmetrical ride-through and grid support in converter-interfaced DG units under unbalanced conditions. IEEE Trans Ind Electron 66(2):1130–1141
13. Alepuz S et al (2009) Control strategies based on symmetrical components for grid-connected converters under voltage dips. IEEE Trans Ind Electron 56(6):2162–2173
14. Du X, Wu Y, Gu S, Tai HM, Sun P, Ji Y (2016) Power oscillation analysis and control of three-phase grid-connected voltage source converters under unbalanced grid faults. IET Power Electron 9(11):2162–2173
15. Mirhosseini M, Pou J, Agelidis VG (2015) Individual phase current control with the capability to avoid overvoltage in grid-connected photovoltaic power plants under unbalanced voltage sags. IEEE Trans Power Electron 30(10):5346–5351
16. Jiang W, Wang Y, Hang H, Zheng Z, Wang L (2016) Coordinated instantaneous active power control for PWM rectifier under grid voltage dips considering the limitation of phase current. Zhongguo Dianji Gongcheng Xuebao/Proc Chin Soc Electr Eng 36(22):6220–6230
17. Guo X, Zhang X, Wang B, Wu W, Guerrero JM (2014) Asymmetrical grid fault ride-through strategy of three-phase grid-connected inverter considering network impedance impact in low-voltage grid. IEEE Trans Power Electron 29(3):1064–1068
18. Borrell Á, Velasco M, Castilla M, Miret J, Guzmán R (2022) Collaborative voltage unbalance compensation in islanded AC microgrids with grid-forming inverters. IEEE Trans Power Electron 37(9):10499–10513
19. Wang X, Wang C, Tao Xu, Guo L, Li P, Li Yu, Meng He (2018) Optimal voltage regulation for distribution networks with multi-microgrids. Appl Energy 210:1027–1036
20. Peng Y, Shuai Z, Guerrero JM, Li Y, Luo A, Shen ZJ (2020) Performance improvement of the unbalanced voltage compensation in islanded microgrid based on small-signal analysis. IEEE Trans Industr Electron 67(7):5531–5542
21. Pavankumar Y, Debnath S, Paul S (2023) Multi-objective pareto optimal unbalance voltage compensation in the microgrid. Electr Power Syst Res 217:109104
22. Camacho A, Castilla M, Miret J, De Vicuna LG, Guzman R (2018) Positive and negative sequence control strategies to maximize the voltage support in resistive-inductive grids during grid faults. IEEE Trans Power Electron 33(6):5362–5373
23. Ji L, Shi J, Hong Q, Fu Y, Chang X (2021) A multi-objective control strategy for three phase grid-connected inverter during unbalanced. IEEE Trans Power Del 36(4):2490–2500
24. Ghahderijani MM, Camacho A, Moreira C, Castilla M, De Vicuña LG (2020) Imbalance-voltage mitigation in an inverter-based distributed generation system using a minimum current-based control strategy. IEEE Trans Power Del 35(3):1399–1409
25. Çelik D, Meral ME (2020) Multi-objective control scheme for operation of parallel inverter-based microgrids during asymmetrical grid faults. IET Renew Power Gener 14(13):2487–2498. https://doi.org/10.1049/iet-rpg.2020.0057
26. Zarei SF, Mokhtari H, Ghasemi MA, Peyghami S, Davari P, Blaabjerg F (2020) Control of grid-following inverters under unbalanced grid conditions. IEEE Trans Energy Conv 35(1):184–192